Acta Cryst. (1986). B42, 17-21

A HREM Study of the Superstructures of Ferrifayalite

BY B. S. ZOU AND K. H. KUO

Institute of Metal Research, Academia Sinica, 110015 *Shenyang, People's Republic of China*

(*Received* 10 *June* 1985; *accepted* 28 *August* 1985)

Abstract

The structure of ferrifayalite and its three superstructures have been studied by high-resolution electron microscopy. The match between through-focus images and simulated ones verifies the result of X-ray structural analysis: ferrifayalite is a new Fe^{3+}-rich silicate mineral with space group $P2_1/b$, $Z=4$, and the chemical formula $Fe^{3+}Fe^{2+}_{0.5}SiO_4$. The frequent appearance of superlattice reflections, such as $00\frac{1}{3}$, $00\frac{1}{2}$ and $00\frac{2}{3}$ along the **c*** direction of ferrifayalite, implies the presence of superstructures which is due to an ordering of Fe^{2+} ions. Various structure models based on the observed structure images have been proposed for these three superstructures.

1. Introduction

Since 1976 a new mineral of the ferrifayalite group has been found in several places in China and it has been called laihunite because it was first found in the village Laihu of Liaoning province. This mineral has semimetallic luster and weak ferromagnetism. It is an orthosilicate with approximate composition $Fe^{3+}Fe^{2+}_{0.5}SiO_4$. Previous X-ray studies have revealed a monoclinic unit cell with $a=4{\cdot}812$, $b=10{\cdot}211$, $c=5{\cdot}813$ Å, $\alpha=90{\cdot}87°$, $Z=4$ and space group $P2_1/b$ (Fu, Kong & Zhang, 1979; in order to facilitate comparison with fayalite a was chosen as the unique axis). Compared with fayalite $Fe^{2+}_2SiO_4$, this ferrifayalite seems to be an oxidation product having some Fe^{2+} vacancies in the octahedral sites surrounded by O^{2-} ions.

Both X-ray and electron diffraction have sometimes shown superlattice spots such as $00\frac{1}{3}$, $00\frac{1}{2}$ and $00\frac{2}{3}$ implying the existence of superstructures in this ferrifayalite. In fact, some fringes with a spacing equal to $2c$, $3c$, or $1{\cdot}5c$ have also been observed in lattice images (Li, Liu, Kong & Fu, 1981; Kitamura, Shen, Banno & Morimoto, 1984). A superstructure with $3c$ has been studied recently in detail by single-crystal diffractometry and the ordering of Fe^{2+} vacancies in it has been determined (Shen, Tamada, Kitamura & Morimoto, 1982).

In the present study the structure of ferrifayalite and its three superstructures have been studied by means of high-resolution electron microscopy (HREM) and various structure models with an ordered distribution of vacancies have been proposed for these three superstructures.

2. Structure image of ferrifayalite

Crystallites of this mineral were first crushed in an agate mortar and then placed on holey carbon films. They were examined in a JEM-200CX electron microscope equipped with a top-entry goniometer stage ($C_s=1{\cdot}2$ mm) having an interpretable point resolution of 0·25 nm. Various crystals with the [uv0] orientations were chosen so that the image always includes [001], which makes it easy to identify superstructures with a c parameter equal to several times that of the ferrifayalite. All high-resolution images were taken with symmetrical incidence.

The structure model of ferrifayalite projected on (100) is shown in Fig. 1. Owing to the presence of Fe^{3+} ferric ions, vacancies are created in the octahedral sites of Fe^{2+} ferrous ions at $00\frac{1}{2}$ and $\frac{1}{2}\frac{1}{2}\frac{1}{2}$. The atomic coordinates determined by the X-ray diffraction method are given in Table 1, which will be used later in image simulations.

Simulated images were calculated based upon the multislice program written by Ishizuka (1982). The parameters used for the image simulation are: the half-width of a Gaussian spread of focus Δ at the experimental gun bias (70 Å); the semi-angle of convergence of the incident beam ($\theta_c/\lambda=0{\cdot}030$ rad Å^{-1}); and the size limited by the objective aperture ($\sin\theta/\lambda=0{\cdot}35$ Å^{-1}).

Fig. 2 shows a through-focus series of [110] structure images of ferrifayalite. Here the simulated images

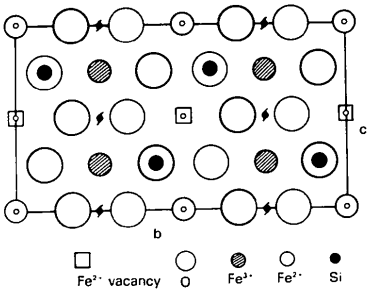

Fig. 1. Structure of ferrifayalite projected on (100). Ordered vacancies of Fe^{2+} ions occur at positions $00\frac{1}{2}$ and $\frac{1}{2}\frac{1}{2}\frac{1}{2}$.

0108-7681/86/010017-05$01.50

are calculated at a thickness of 220 Å using 39 waves. The correspondence between the observed and simulated images is sufficiently good to warrant a correct interpretation of the observed image taken at the Scherzer defocus $\Delta f = -600$ Å. Fig. 3 is such an image. An electron diffraction pattern, a structure model and a simulated image are shown as insets. The white circle in the electron diffraction pattern corresponds to the size of aperture used in imaging. The bright dots in the observed and simulated images accord with each other not only in position but also in orientation. The bright dots also correspond very well to the tunnels formed by the zigzag chains of Fe atoms. Such a good correspondence in the case of the well established structure of ferrifayalite suggests that the structure image taken at the Scherzer defocus could be used to interpret the superstructure of ferrifayalite.

3. Superstructures with ordered vacancies

3.1. *Superlattice reflections*

As mentioned above, superlattice reflections along the **c*** direction occur frequently in ferrifayalite implying the presence of ordered vacancies with a period several times that of the fundamental unit cell. Fig. 4 shows the $00l$ row of reflections from the fundamental structure as well as those from three superstructures. There are fractional spots at $\frac{1}{3}$ and $\frac{1}{2}$ in Figs. 4(b) and 4(c), respectively, and both fractional spots are present in Fig. 4(d). We call these three superstructures $3C_1$, $2C$ and $3C_2$.

Table 1. *Atomic coordinates in the fundamental structure of ferrifayalite*

Ions or atoms	Number	x	y	z
Fe^{2+}	2	0	0	0
Fe^{3+}	4	0	0·274	0·740
Si	4	0·060	0·403	0·243
O(1)	4	0·298	0·055	0·239
O(2)	4	0·245	0·076	0·753
O(3)	4	0·722	0·166	0·526
O(4)	4	0·230	0·337	0·030

3.2. $3C_1$ *superstructure*

This superstructure has been studied in great detail by X-ray single-crystal diffractometry (Shen *et al.*, 1982), giving the following results: (1) $\frac{111}{222}$ and its equivalent sites are only half filled with Fe^{2+}; (2) $\frac{111}{226}$ and its equivalent sites are entirely vacant; (3) 000 and its equivalent sites are completely filled with Fe^{2+}; (4) $00\frac{1}{3}$ and its equivalent sites are completely or partially filled. However, in order to comply with the formula of ferrifayalite $Fe^{3+}Fe^{2+}_{0.5}SiO_4$, where the first three positions are filled, the fourth positions can only be filled with $\frac{3}{4}$ occupancy as shown in Fig. 5(b). The period of $3c$ can be detected in the structure

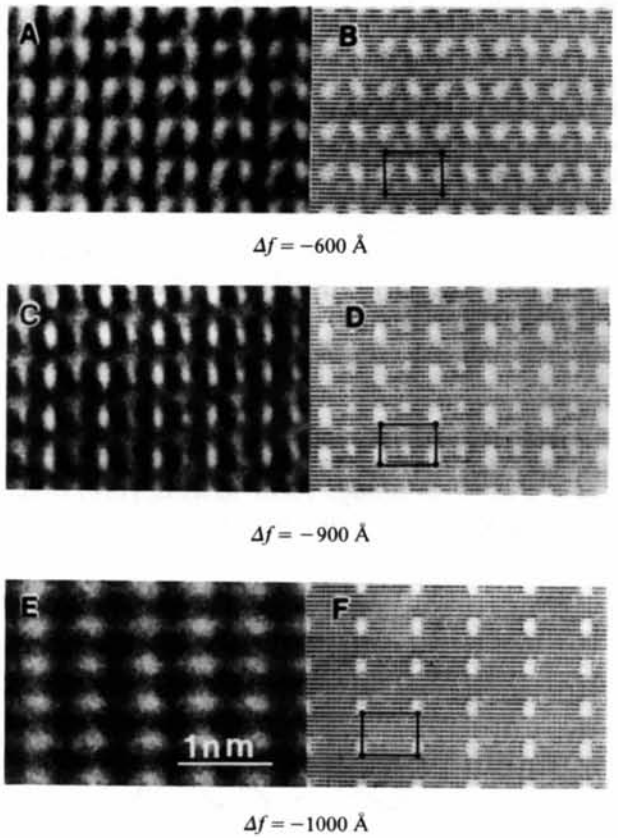

Fig. 2. The through-focus series of the [110] structure and simulated images of ferrifayalite at a thickness of 220 Å. The unit cell is drawn in the simulated images. (1 nm = 10 Å.)

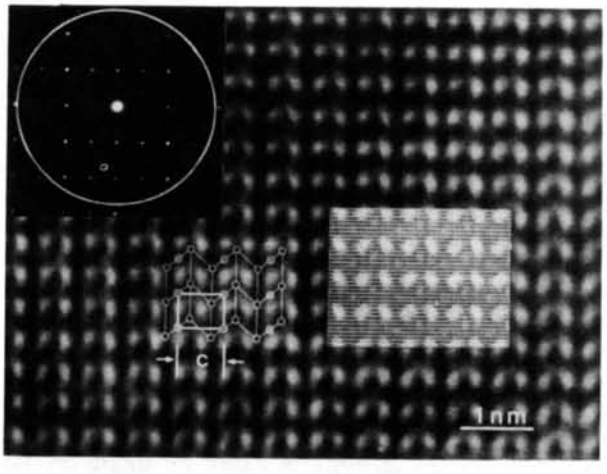

Fig. 3. The [110] structure image of ferrifayalite at the Scherzer defocus taken using the electron beams within the white circle in the top-left electron diffraction pattern. Open and double circles are Fe^{3+} and Fe^{2+} ions respectively. The bright dots correspond to the tunnels surrounded by these metal ions. An inserted simulated image accords fairly well with the observed one.

image (Fig. 6) and the agreement between the bright dots in the observed and simulated images supports the X-ray determination of the distribution of Fe^{2+} in the octahedral site (Shen *et al.*, 1982). The simulated images shown in Fig. 6 are calculated with 119 waves at a crystal thickness of 9 nm assuming symmetrical incidence. However, this kind of superperiod cannot be observed at the thin edge of the crystallites and the calculation has confirmed that it is only recognizable when the thickness of the crystallite reaches 200–400 Å. This is because the amplitude of the superlattice reflection $00\frac{1}{3}$ increases noticeably with thickness and becomes comparable with the fundamental reflection 001 at a thickness of 200–400 Å (Fig. 7) yielding the detectable contrast on the image.

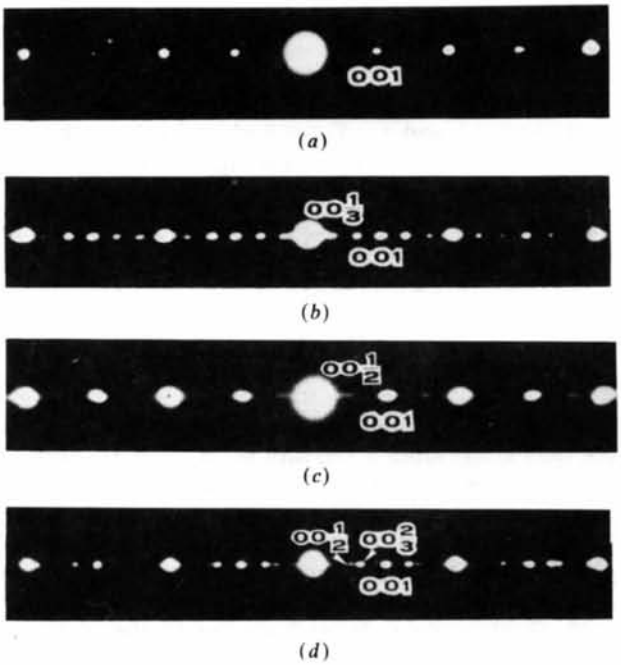

Fig. 4. The $00l$ row of diffraction spots of (*a*) ferrifayalite and of the three superstructures: (*b*) $3C_1$, (*c*) $2C$ and (*d*) $3C_2$. Fractional spots at $00\frac{1}{3}$, $00\frac{1}{2}$ and $00\frac{2}{3}$ correspond to the superlattice reflections of these superstructures.

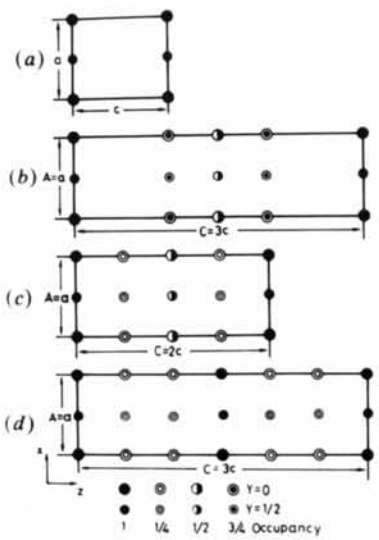

Fig. 5. [010] projected structure models showing occupancy of Fe^{2+} ions in (*a*) ferrifayalite and its three superstructures: (*b*) $3C_1$, (*c*) $2C$ and (*d*) $3C_2$.

3.3. $2C$ *superstructure*

Although the superstructure with a period of twice c has been noticed either by the occurrence of the $00\frac{1}{2}$ reflection or by the appearance of lattice fringes with a spacing of 12 Å (Li *et al.*, 1981; Shen *et al.*, 1982), the distribution of Fe^{2+} ions has not been determined. Since each supercell has eight $Fe^{3+}Fe^{2+}_{0.5}SiO_4$, there should be four Fe^{2+} ions. As shown in Fig. 5(*c*), the Fe^{2+} positions in this superlattice can be divided into three sets: 000, $00\frac{1}{4}$, $00\frac{1}{2}$. If the occupancy of these sets is limited to 0, $\frac{1}{4}$, $\frac{1}{2}$, $\frac{3}{4}$ or

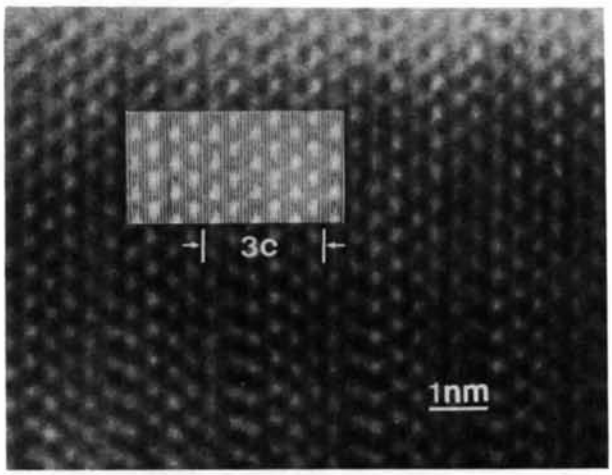

Fig. 6. The [110] structure image of the $3C_1$ superstructure taken at the Scherzer defocus. The inset shows a simulated image. The $3c$ fringes are marked with arrows.

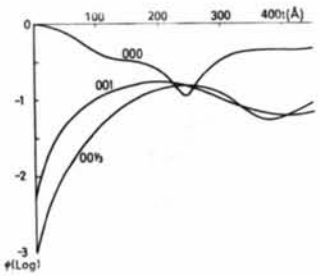

Fig. 7. Variation of diffraction amplitudes of transmitted 000, fundamental 001 and superlattice $00\frac{1}{3}$ beams with crystal thickness for the $3C_1$ superstructure. At 200 Å these beams have comparable magnitudes.

Table 2. *Four different combinations of the distributions of* Fe^{2+} *ions in the 2C superstructure of ferrifayalite*

	000			$00\frac{1}{4}$			$00\frac{1}{2}$			
No.	No. of sites	Occupancy	Fe^{2+}	No. of sites	Occupancy	Fe^{2+}	No. of sites	Occupancy	Fe^{2+}	Total Fe^{2+} ions
1	2	1	2	4	$\frac{1}{2}$	2	2	0	0	4
2	2	1	2	4	$\frac{1}{4}$	1	2	$\frac{1}{2}$	1	4
3	2	$\frac{3}{4}$	$\frac{3}{2}$	4	$\frac{1}{2}$	2	2	$\frac{1}{4}$	$\frac{1}{2}$	4
4	2	$\frac{1}{2}$	1	4	$\frac{3}{4}$	3	2	0	0	4

1, then there are only four different combinations to maintain the formula $Fe^{3+}Fe^{2+}_{0.5}SiO_4$ and the space group $P2_1/b$. These four different combinations of Fe^{2+} occupancy are shown in Table 2.

Simulated images were calculated for these four different ordered vacancies with varying defocus and thickness. It was found that the simulated image based on the second model in Table 2 which has been shown in Fig. 5(*c*) shows the best agreement with the observed one. Fig. 8 shows the [120] structure image, where the inset was calculated with 43 waves at a crystal thickness of 168 Å. In this [120] structure image, the 2*c* superstructure can be clearly seen.

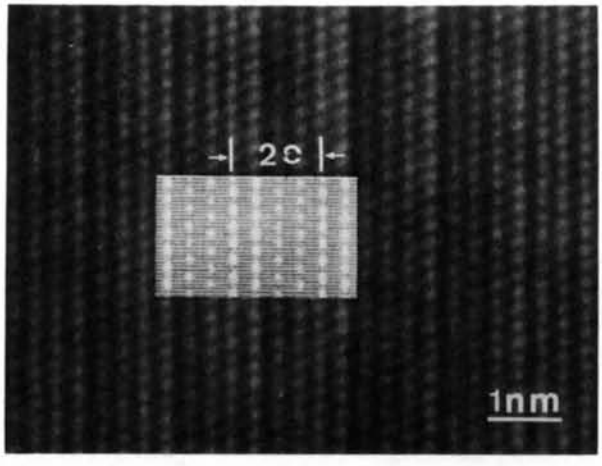

Fig. 8. The [120] structure image of the 2*C* superstructure taken at the Scherzer defocus. The inset shows a simulated image. The 2*c* fringes are marked with arrows.

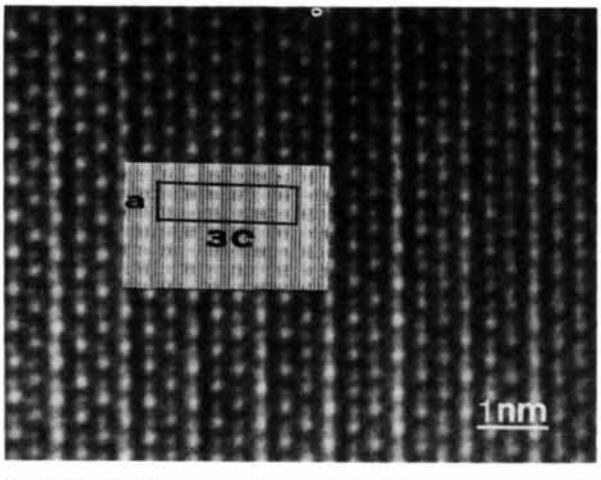

Fig. 9. The [010] structure image of the $3C_2$ superstructure taken at the Scherzer defocus. The inset shows a simulated image. The 1·5*c* fringes with a stronger contrast can clearly be seen.

3.4. $3C_2$ *superstructure*

The fractional superlattice reflections at $00\frac{1}{2}$ and $00\frac{2}{3}$ may come from a mixture of 2*C* and 3*C* superstructures. In fact, the high-resolution images taken in this case clearly show the coexistence of 2*C* and 3*C* superstructures. When this high-resolution micrograph is used as the object in an optical diffractometer, the optical diffraction pattern formed at the back focal plane is indeed similar to the electron diffraction pattern shown in Fig. 4(*d*). Here the 3*C* superstructure is denoted as $3C_2$ in order to differentiate it from the $3C_1$ superstructure. The $3C_2$ superstructure has the following two distinctive features. First, no $00\frac{1}{3}$ superlattice reflection has been observed. Secondly, the lattice fringes show a spacing of 1·5*c*, instead of 3*c*, which corresponds to the fractional reflections $00\frac{2}{3}$. These features imply that the distribution of Fe^{2+} ions has a period of 1·5*c*, as in the proposed structure model in Fig. 5(*d*). In this 1·5*c* supercell, Fe^{2+} ions can only occupy two sets of positions, namely 000 and $00\frac{1}{3}$ ($00\frac{1}{6}$ in the $3C_2$ supercell). There are only two combinations of Fe^{2+} occupancy: (1) full occupancy at 000; $\frac{1}{4}$ occupancy at $00\frac{1}{3}$; (2) full vacancy at 000; $\frac{3}{4}$ occupancy at $00\frac{1}{3}$. The first combination gives a simulated image which has better correlation with the observed one.

However, the supercell can only be an integral multiple of the fundamental cell, when other ions such as Fe^{3+}, O^{2-}, Si^{4+} are taken into consideration. In other words, the real period of the superstructure is not 1·5*c* but 3*c*. The occupancies of four sets of Fe^{2+} are: 1 at 000 and $00\frac{1}{2}$; $\frac{1}{4}$ at $00\frac{1}{6}$ and $00\frac{1}{3}$, as shown in Fig. 5(*d*). The [010] structure image and a simulated one are shown in Fig. 9. Here strong contrast with a period of 1·5*c* is very obvious. The simulated image was calculated with 135 waves at a crystal thickness of 102 Å.

We would like to thank Dr A. Olsen for many stimulating discussions and Professor H. Hashimoto for reviewing the manuscript.

References

FU, P. Q., KONG, Y. H. & ZHANG, L. (1979). *Geochimica*, No. 2, pp. 103-119 (in Chinese).

ISHIZUKA, K. (1982). *Acta Cryst.* A**38**, 773-779.

KITAMURA, M., SHEN, B. M., BANNO, S. & MORIMOTO, N. (1984). *Am. Mineral.* **69**, 154-160.

LI, F. H., LIU, W., KONG, Y. H. & FU, P. Q. (1981). *Kexue Tongbao*, **10**, 590-592 (in Chinese).

SHEN, B. M., TAMADA, O., KITAMURA, M. & MORIMOTO, N. (1982). *Sci. Geol. Sin.* No. 3, pp. 341-342 (in Chinese).

Acta Cryst. (1986). B**42**, 21-25

A New Intermetallic Tetrahedrally Close-Packed Structure with Juxtaposed Pentagonal Antiprisms Determined by High-Resolution Electron Microscopy

BY D. N. WANG, H. Q. YE AND K. H. KUO

Institute of Metal Research, Academia Sinica, 110015 *Shenyang, People's Republic of China*

(*Received* 7 *January* 1985; *accepted* 7 *June* 1985)

Abstract

A new intermetallic tetrahedrally close-packed phase, called the C phase, was found coexisting with the $C14$ Laves phase by means of high-resolution electron microscopy and selected-area electron diffraction. Its space group and lattice parameters are: $B2/m$, $a = 17{\cdot}8$, $b = 7{\cdot}7$, $c = 4{\cdot}7$ Å, $\gamma = 99°$ and $Z = 50$ (e.s.d.'s of lattice parameters *ca* 0·05 Å). Its atomic coordinates and orientation relationships with the $C14$ Laves phase have also been determined.

1. Introduction

A number of tetrahedrally close-packed (t.c.p.) phases, such as σ, μ, Laves, *etc.*, are known to exist in many binary and ternary alloys of transition metals as well as in many industrial steels and superalloys. Frank & Kasper (1959) have shown that these t.c.p. structures consist of juxtaposed hexagonal (*e.g.* σ) or pentagonal (*e.g.* μ and Laves phases) antiprisms. In the former case, a number of new phases have recently been found coexisting with the σ phase and their structures have been inferred from high-resolution electron images (Ye & Kuo, 1984; Ye, Li & Kuo, 1984; Li & Kuo, 1986). One of these phases has also been determined by the convergent-beam electron diffraction technique (Lin & Steeds, 1986). Since these phases occurred in intimate intergrowth with σ and also with each other and their dimensions seldom exceeded 1 μm, high-resolution electron microscopy (HREM) and selected-area electron diffraction (SAD) seem to be the only measures one can take to solve their structures.

The t.c.p. structures with juxtaposed pentagonal antiprisms in general (Ye, Li & Kuo, 1985) and the domain structure of the $C14$ Laves phase in particular (Ye, Wang & Kuo, 1985*a*) have recently been discussed. It was shown that when faults occur in $(1\bar{1}\bar{1})$ or $(1\bar{1}0)$ in the $C14$ Laves phase, single slabs of μ structure are generated at the domain boundaries (Fig. 1) and if such faults occur periodically on every other $(1\bar{1}\bar{1})$ or $(1\bar{1}0)$ plane a structure consisting of alternate μ and $C14$ Laves slabs will result. This structure is similar to the C silicide $V_2(Co_{0.57}Si_{0.43})_3$ reported earlier (Bardos & Beck, 1966; Kripyakevich & Yarmolyuk, 1971) and it is therefore simply called the C phase and occurs generally in intimate intergrowth with the heavily faulted $C14$ Laves phase (Fig. 2). The structure of this C phase and its orientation relationships with the $C14$ Laves phase have been studied by means of HREM and SAD and the results are presented in the following.

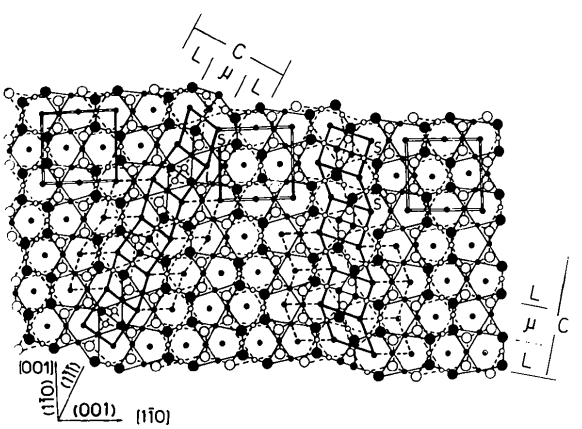

Fig. 1. A schematic diagram illustrating slabs of the C phases generated from the $(1\bar{1}\bar{1})$ and $(1\bar{1}0)$ faults in the $C14$ Laves phase projected on the (110) plane.

0108-7681/86/010021-05$01.50